Scaling and Modeling of Three-Dimensional, Pressure-Driven Turbulent Boundary Layers

U. Goldberg* and E. Reshotko†
Case Western Reserve University, Cleveland, Ohio

The method of matched asymptotic expansions is employed to find the various subregions in three-dimensional, pressure-driven turbulent boundary layers, and to identify the proper scaling of these regions. Based on the results of this analysis, models are proposed for the three-dimensional law of the wall and law of the wake. Comparisons between these models and the data of van den Berg et al. and Mueller show good agreement between theory and experiments.

Nomenclature

A = parameter used in Johnston's triangular model
A' = variable used in the law of the wake, $=2\kappa^{-1}\Pi$
B = constant used in the logarithmic overlap region, $\cong 5.0$
C_f = skin friction coefficient, $=2\tau_w/\rho\tilde{U}_\infty^2$
F = defect function used in the law of the wake
l = length scale ($=\lambda\delta$)
P = pressure
Q = outer variable (stands for U_i, P, T_{ij})
q = middle-layer variable (stands for u_i, p, t_{ij})
$\hat{q}$ = inner variable (stands for $\hat{u}_i, \hat{p}, \hat{t}_{ij}$)
Re_l = Reynolds number based on l, $=\tilde{U}_e l/\nu$
Re_δ = Reynolds number based on δ, $=\tilde{U}_e\delta/\nu$
Re_{δ^*} = Reynolds number based on δ^*, $=\tilde{U}_e\delta^*/\nu$
T_{ij} = Reynolds stress, $=-\overline{\tilde{u}_i'\tilde{u}_j'}/u_\tau^2$
U = resultant velocity
U_x = streamwise velocity component
U_p = U at apex in Johnston's triangle
U_y = normal velocity component
U_z = cross-flow velocity component
u^* = velocity perturbation scale
u_τ = friction velocity, $=[\tau_w/\rho]^{1/2}$
u^+ = law-of-the-wall velocity, $\tilde{U}/u_\tau$
X, Y, Z = streamwise, normal, and crosswise coordinates, respectively
y = normal coordinate in middle layer, $=Y/\epsilon$
$\hat{y}$ = normal coordinate in inner layer, $=Y/\epsilon\hat{\epsilon}$
y^+ = law-of-the-wall normal coordinate, $=\tilde{Y}u_\tau/\nu$
α, β = parameters appearing in Eq. (10)
β_e = external flow direction relative to direction at upstream position
Γ = wake variable, $=\gamma/\gamma_m$
γ = angle appearing in polar plot of U_z vs U_x
γ_m = value of γ at outer edge of defect layer
δ = boundary-layer thickness
δ^* = displacement thickness
ϵ = normal length scale of defect layer, $=u_\tau/\tilde{U}_e$
$\epsilon\hat{\epsilon}$ = normal length scale of inner layer, $=\epsilon^{-1}Re_l^{-1}$
η = normalized normal coordinate, $=\tilde{Y}/\delta$
κ = von Kármán constant, $\cong 0.41$
λ = $[2/C_f]^{1/2}$
ν = kinematic viscosity
Π = wake parameter
ρ = density
τ = shear stress
ϕ = angle between U and U_x in polar plot of U_z vs U_x

Superscripts

$(\tilde{\ })$ = dimensional quantity
$(\hat{\ })$ = inner layer variable

Subscripts

e = evaluated at the local freestream
m = maximum value
w = evaluated at the wall
x, z = X- and Z-wise quantities, respectively
0 = evaluated at the point where the wall and wake velocity vectors are in the same direction
1 = evaluated at the point of switching from the logarithmic overlap to the wake
2D = two-dimensional flow
∞ = evaluated at the upstream position

Introduction

THREE-DIMENSIONAL, pressure-driven turbulent boundary layers occur in both external and internal flows. Examples are the boundary layers on swept wings and on turbomachinery endwalls between compressor blades or turbine blades. Gaining physical understanding of this type of flow is, therefore, very important both for analysis and design purposes.

The present work attempts to point out some basic physics of such flows and suggests models which attempt to describe these flows analytically.

Coles[1] was apparently the first to suggest the possibility of treating three-dimensional turbulent boundary layers in vector form, whereby the entire velocity profile is described by the sum of two vectors: wall and wake components. Based on the experimental data available to him, Coles tentatively stated that if the wall component is in the direction of the surface shear stress, then the wake component would be very nearly parallel to the direction of the pressure gradient.

Johnston[2] suggested the approach of treating the secondary (or crosswise) component of a three-dimensional turbulent boundary layer as a function of the main (or streamwise) component and certain additional parameters. He was thus led through examination of data to the proposition of his well-known triangular model to describe the form of the velocity hodograph. Based on his own experiments and those of others, Johnston suggested two explicit relationships to

Received July 12, 1983; presented as Paper 83-1695 at the AIAA 16th Fluid and Plasma Dynamics Conference, Danvers, Mass., July 12-14, 1983; revision received Nov. 8, 1983.

*Graduate Student, Department of Mechanical and Aerospace Engineering. Currently at AVCO Systems Div., Wilmington, Mass. Member AIAA.

†Professor, Department of Mechanical and Aerospace Engineering. Fellow AIAA.

Table 1 Momentum equation in the three sublayers to orders 1, ϵ, and ϵ^2

Outer region	Middle region	Inner region
	Order 1	
Euler equations (No Reynolds stresses)	$p_1 = P_1(X,0,Z)$ Euler equations	$\hat{p}_1 = P_1(X,0,Z)$ $\hat{u}_{x_1} = \hat{u}_{y_1} = \hat{u}_{z_1} = 0$
	Order ϵ	
$U_{x_2} = U_{y_2} = U_{z_2} = 0$ $P_2 = 0$	$p_2 = 0$ Boundary-layer equations. Reynolds stresses only	$\hat{p}_2 = 0$ Constant total shear across sublayer
	Order ϵ^2	
Euler equations	Full Navier-Stokes equations for X- and Z-momenta Reynolds stresses only	$\hat{p}_3 = P_3(X,0,Z) + \hat{t}_{1_{yy}}$ Constant total shear across sublayer

describe the triangular model: one for the region adjacent to the wall and the other for the region near the freestream. His model is successful enough in the regions away from the vertex of the triangle but fails to match the data adequately in the vicinity of the vertex. As will be shown later, this region corresponds to the transitional region from the wall sublayer to the wake sublayer. In spite of its relative success, Johnston's model suffers from being a product of data correlation without the benefit of a supporting analysis.

In order to gain a better understanding about the physics of three-dimensional, pressure-driven turbulent boundary layers, it became clear that some analysis would be helpful. To this end, Mellor's[3] two-dimensional asymptotic analysis for large Reynolds number turbulent boundary layers has been extended to three dimensions in the present work. The results of this analysis provide the scaling of a three-dimensional boundary layer as well as the main features that a three-dimensional law-of-the-wall and law-of-the-wake model should possess. Based on these indications, composite wall and wake laws are herein proposed, utilizing a vector approach in the wake region. This model is then compared with van den Berg and Elsenaar's et al.[4,5] infinite swept wing flow data and Mueller's[6,7] forced turning flow data with good agreement, suggesting the apparent validity of the present approach, at least for fully attached flows. It should be mentioned that Johnston's triangle emerges as a particular case of the present model.

Asymptotic Analysis

A typical skewed boundary layer and basic nomenclature are shown in Fig. 1. For incompressible steady flow with no curvatures, the mean part of a turbulent flow is described by the following equations:

Mass conservation:

$$\frac{\partial U_i}{\partial X_i} = 0 \tag{1}$$

Momentum:

$$U_j\left(\frac{\partial U_i}{\partial X_j}\right) = -\frac{\partial P}{\partial X_i} + \frac{\partial}{\partial X_j}\left(\epsilon^2 T_{ij} + \epsilon^2 \hat{\epsilon}\frac{\partial U_i}{\partial X_j}\right) \tag{2}$$

where

$$U_i = \tilde{U}_i/\tilde{U}_e, \quad P = \tilde{P}/\rho\tilde{U}_e^2, \quad T_{ij} = -\overline{\tilde{u}_i'\tilde{u}_j'}/u^{*2}$$

$$X_i = \tilde{X}_i/l, \quad \epsilon = u^*/\tilde{U}_e, \quad \epsilon^2\hat{\epsilon} = \nu/(\tilde{U}_e l) = Re_l^{-1}$$

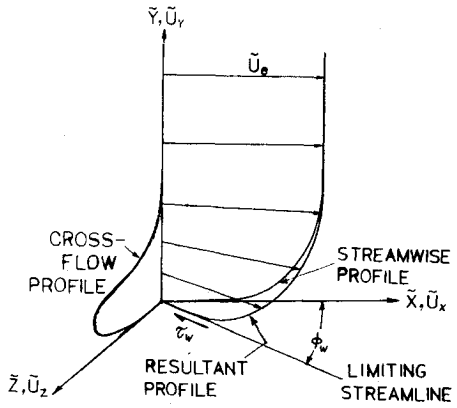

Fig. 1 Skewed boundary layer and basic terminology.

In the above equations, ϵ^2 is the scale for the Reynolds stresses, with u^* being an as yet undetermined perturbation velocity scale. $\epsilon^2\hat{\epsilon}$ is the scale for the viscous stresses, which is also given by Re_l^{-1}. Thus $\hat{\epsilon}$ is the relative magnitude of viscous to Reynolds stresses.

In addition, the following boundary conditions are required:

$$U_i(X,0,Z) = 0$$

and, assuming a uniform external flow,

$$\begin{Bmatrix} U_x \\ U_z \end{Bmatrix}(X,\infty,Z) = \begin{Bmatrix} 1 \\ 0 \end{Bmatrix}$$

for a fixed (X,Z) location.

Next, an asymptotic analysis is carried out (following Mellor[3]) for the above equations, using the following expansions.

Outer Expansion

$$Q = Q_1 + \epsilon Q_2 + \epsilon^2 Q_3 + \ldots, \quad T_{ij} = 0$$

where Q stands for the three velocity components and pressure:

$$Q = (U_x(X,Y,Z), U_y, U_z, P)\ddagger$$

‡In the present analysis an expression of the form $U(X,Y,Z)$ should be interpreted as $U(Y)$ at a given (X,Z) location.

Middle Expansion

$$y=Y/\epsilon, \quad U_x=u_{x_1}(X,y,Z)+\epsilon u_{x_2}+\epsilon^2 u_{x_3}+\ldots$$

$$U_y=\epsilon(u_{y_1}+\epsilon u_{y_2}+\epsilon^2 u_{y_3}+\ldots), \quad U_z=u_{z_1}+\epsilon u_{z_2}+\epsilon^2 u_{z_3}+\ldots$$

$$P=p_1+\epsilon p_2+\epsilon^2 p_3+\ldots, \quad T_{ij}=t_{1_{ij}}+\epsilon t_{2_{ij}}+\epsilon^2 t_{3_{ij}}+\ldots$$

Inner Expansion

$$\hat{y}=y/\hat{\epsilon}=Y/\epsilon\hat{\epsilon}, \quad U_x=\hat{u}_{x_1}(X,\hat{y},Z)+\epsilon\hat{u}_{x_2}+\epsilon^2\hat{u}_{x_3}+\ldots$$

$$U_y=\epsilon\hat{\epsilon}(\hat{u}_{y_1}+\epsilon\hat{u}_{y_2}+\epsilon^2\hat{u}_{y_3}+\ldots), \quad U_z=\hat{u}_{z_1}+\epsilon\hat{u}_{z_2}+\epsilon^2\hat{u}_{z_3}+\ldots$$

$$P=\hat{p}_1+\epsilon\hat{p}_2+\epsilon^2\hat{p}_3+\ldots, \quad T_{ij}=\hat{t}_{1_{ij}}+\epsilon\hat{t}_{2_{ij}}+\epsilon^2\hat{t}_{3_{ij}}+\ldots$$

These expansions are substituted into Eqs. (1) and (2) and the analysis proceeds in the manner of matched asymptotic expansions. The features of the resulting equations in the three regions are summarized in Table 1 to the first three orders. The main features of the flow, as indicated in the table, are the following: the outer layer is inviscid; the middle layer is influenced by Reynolds stresses to orders 2 and 3, where the second-order equations are of the boundary-layer type while the third-order ones are full Navier-Stokes equations; the inner layer is dominated by constant total shear (viscous plus Reynolds stresses) across it, with no pressure gradient or inertia effects through order 3. The important information for the subsequent analysis is contained in the first-order outer-region equations and in the second-order middle- and inner-region equations.

As a result of the asymptotic analysis and the matching procedure, the following conclusions emerge:

1) The flow possesses a three-layer structure.

2) The inner and middle layers have a common logarithmic overlap.

3) The inner layer is exponentially thin compared to the middle layer:

$$\hat{\epsilon}=O(e^{-1/\epsilon}) \text{ as } \epsilon\to 0$$

4) The pressure gradient does not influence the inner layer, hence the wall shear stress is the only driving force there. Thus the flow is two-dimensional in the inner layer and the velocity vectors are coplanar in the τ_w direction.

5) Since the outer flow is in the freestream direction, all the turning from the τ_w direction to the $\tilde{U}_e$ direction must take place in the middle layer.

While the first three conclusions apply also to two-dimensional boundary layers, the last two are special to the three-dimensional case.

Profile Relations

Based on these results, the general forms for the law of the wall and law of the wake are the following.

Law of the wall:

$$u^+(y^+)=\tilde{U}(\tilde{X},\tilde{Y},\tilde{Z})/u_\tau(\tilde{X},\tilde{Z})$$

where

$$y^+=\tilde{Y}u_\tau/\nu, \quad u_\tau=(\tau_w/\rho)^{1/2}$$

Law of the wake

$$F(\tilde{X},\eta,\tilde{Z})=\frac{\tilde{U}_e(\tilde{X},\tilde{Z})-\tilde{U}(\tilde{X},\tilde{Y},\tilde{Z})}{u_\tau(\tilde{X},\tilde{Z})}$$

where

$$\eta=\tilde{Y}/\delta$$

Matching these two laws yields the logarithmic overlap:

$$F(\tilde{X},\eta,\tilde{Z})\sim-\kappa^{-1}\ell n\eta+A', \quad \eta\to 0$$

$$u^+(y^+)\sim\kappa^{-1}\ell n y^+ + B, \quad y^+\to\infty$$

where

$$\kappa\cong 0.41, \quad B\cong 5.0, \quad A'=2\kappa^{-1}\Pi$$

which are Coles' parameters.

If u^* is now chosen as u_τ then the relationships between F and u^+ on the one hand, and the second-order middle and inner variables on the other, become:

$$F=-(u_{x_2}^2+u_{z_2}^2)^{1/2}, \quad \eta=y; \quad u^+=(\hat{u}_{x_2}^2+\hat{u}_{z_2}^2)^{1/2}, \quad y^+=\hat{y}$$

This enables the construction of the composite velocity profile, following the general scheme

$$\left\{\begin{matrix}\text{composite}\\ \text{profile}\end{matrix}\right\}=(\text{outer profile})-(\text{common outer}$$

$$-\text{middle asymptote})+(\text{middle profile})-(\text{common middle}$$

$$-\text{inner asymptote})+(\text{inner profile})$$

Written out explicitly, the composite profile, to order ϵ, has the form:

$$\left\{\begin{matrix}U_x\\ U_z\end{matrix}\right\}=\left\{\begin{matrix}u_{x_1}\\ u_{z_1}\end{matrix}\right\}(X,\eta,Z)+\left[\left\{\begin{matrix}U_{x_1}\\ U_{z_1}\end{matrix}\right\}(X,Y,Z)\right.$$

$$\left.-\left\{\begin{matrix}U_{x_1}\\ U_{z_1}\end{matrix}\right\}(X,0,Z)\right]+\epsilon\left\{-\eta\frac{\partial}{\partial Y}\left\{\begin{matrix}U_{x_1}\\ U_{z_1}\end{matrix}\right\}(X,0,Z)\right.$$

$$-\left\{\begin{matrix}\cos\gamma\\ -\sin\gamma\end{matrix}\right\}F(X,\eta,Z)$$

$$\left.+\left\{\begin{matrix}\cos\phi_w\\ \sin\phi_w\end{matrix}\right\}[-(\kappa^{-1}\ell n y^+ + B)+u^+(y^+)]\right\}$$

where

$$U=(U_x^2+U_z^2)^{1/2}, \quad \phi=\tan^{-1}(U_z/U_x)$$

and γ is the angle between F and U_e. In order to be able to use this profile in actual calculations, it is necessary to provide explicit models for the wall and wake laws.

Law of the Wall

Based on the results of the asymptotic analysis, the wall law is written in the form:

$$u^+=f(y^+), \quad \phi=\phi_w \tag{3}$$

with components

$$u_x^+=u^+\cos\phi_w, \quad u_z^+=u^+\sin\phi_w$$

For f Musker's[8] explicit expression is chosen:

$$f(y^+)=5.424\tan^{-1}\left\{\frac{2y^+-8.15}{16.7}\right\}$$

$$+\log_{10}\left\{\frac{(y^++10.6)^{9.6}}{(y^{+2}-8.15y^++86)^2}\right\}-3.52$$

Law of the Wake

In view of the conclusions from the asymptotic analysis, the wake function is defined in the form:

$$F=(\tilde{U}_e-\tilde{U})/u_\tau$$

with streamwise component

$$F_x=F\cos\gamma=(\tilde{U}_e-\tilde{U}_x)/u_\tau$$

and cross-flow component

$$F_z=-F\sin\gamma=-\tilde{U}_z/u_\tau$$

See Fig. 2 for basic nomenclature.

The two-dimensional defect function may be expressed by Musker's[8] formula

$$F_{2D}=\kappa^{-1}(2\Pi(1-3\eta^2+2\eta^3)-\ell n\eta-\eta^2(1-\eta)) \tag{4}$$

where the wake parameter Π is determinable from[1]

$$2\Pi-\ell n\left\{\frac{1+\Pi}{\kappa Re_{\delta_x^*}}\right\}+\kappa(B-\lambda_x)=0 \tag{5}$$

with

$$\delta_x^*\equiv\int_0^\delta(1-U_x)\,d\tilde{Y}\ \text{and}\ \lambda_x=\left(\frac{2}{C_{f_x}}\right)^{1/2}=\frac{\lambda}{(\cos\phi_w)^{1/2}}$$

There is not an unique generalization of F_{2D} to three dimensions. Possibilities for F_{2D} include:

$$|\tilde{U}_e-\tilde{U}|/u_\tau$$

$$(|\tilde{U}_e|-|\tilde{U}|)/u_\tau$$

$$(\tilde{U}_e-\tilde{U}_x)/u_\tau$$

The first possibility was rejected since it led to poor data correlation; the second is difficult to test or use; the third possibility is the simplest and is the one used henceforth. Thus,

$$F=F_{2D}/\cos\gamma \tag{6}$$

The geometry of Fig. 2 provides the wake law formulation:

$$U=(1-2\lambda^{-1}F\cos\gamma+(\lambda^{-1}F)^2)^{1/2}$$

$$\phi=\tan^{-1}\left\{\frac{\lambda^{-1}F\sin\gamma}{1-\lambda^{-1}F\cos\gamma}\right\} \tag{7}$$

or, equivalently,

$$\tan\gamma=\{(\lambda/F\cos\gamma)-1\}\tan\phi \tag{8}$$

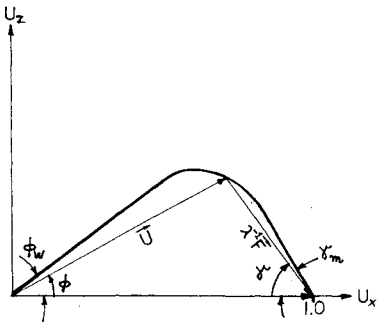

Fig. 2 Hodograph with vector triangle and basic terminology.

In order to complete the formulation of the law of the wake, it is necessary to determine the function $\gamma(\eta)$. Figure 3 shows a plot of experimental values of $\Gamma\equiv\gamma/\gamma_m$, where γ_m is the maximum value of γ. (The data are from Refs. 4 and 6.) It is observed that the lower portion of the plot is different for different stations and that these individual branches merge into a single curve further up. This suggests that Γ could be describable by a combination of two parts, one of which is a function of η and of some physical parameters peculiar to each measurement station, while the other is a function of η only. Pursuing this direction, one arrives at the formulation described below, the details of which are worked out in the Appendix. In the logarithmic overlap region γ is determined from the solution of

$$\frac{d\gamma}{d\eta}=\frac{\lambda\cos^2\gamma}{F_{2D}^2\tan\gamma}\left[\frac{U}{\kappa\eta}-\left(\frac{F_{2D}}{\lambda\cos^2\gamma}-1\right)\frac{dF_{2D}}{d\eta}\right] \tag{9}$$

where U is given by Eq. (7) and F_{2D} by Eq. (4).

The initial condition is

$$\gamma=\gamma_0\ \text{at}\ \eta=\eta_0 \tag{9a}$$

where η_0 is the point where the wake law crosses ϕ_w (see Appendix and Figs. 4 and 5).

In the defect layer, γ is chosen in the form

$$\Gamma\equiv\frac{\gamma}{\gamma_m}=1-\beta(1-\eta)^\alpha \tag{10}$$

as shown in the Appendix, where

$$\alpha=(1-\eta_1)\frac{(d\Gamma/d\eta)_{\eta_1}}{(1-\Gamma_1)},\quad \beta=\frac{(1-\Gamma_1)}{(1-\eta_1)^\alpha} \tag{10a}$$

with subscript 1 denoting the point of switching from the portion of the curve described by Eq. (9) to the one described

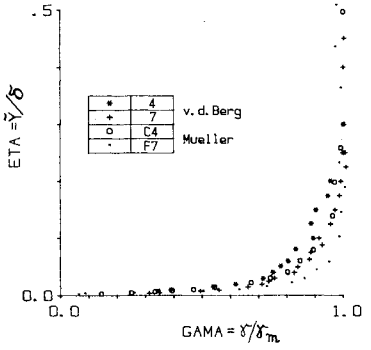

Fig. 3 Typical experimental data of Γ vs η from Refs. 4 and 6.

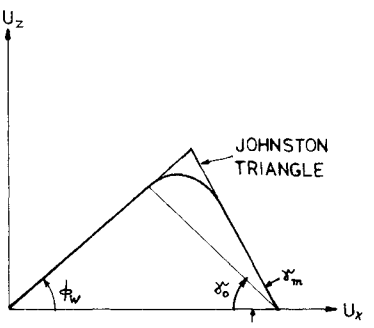

Fig. 4 Hodograph with Johnston's triangle superimposed. Also indicates geometrical significance of γ_0.

by Eq. (10) (see Appendix). The dimensionless distance η_1 is a function of Reynolds number and pressure gradient. A typical value is 0.035. Figure 5 depicts the relation of η_1 to η_0.

At the upper edge of the defect layer γ attains its maximum value, γ_m, which is calculable from[2]

$$\gamma_m = \tan^{-1}\left\{2U_e^2 \int_0^{\beta_e} \frac{d\Psi}{U_e^2}\right\} \tag{11}$$

where β_e is the local freestream direction relative to the direction at the upstream position. The determination of γ_m generally requires knowledge of the external flowfield. Figure 6 depicts a typical comparison between the above model for γ and experimental data.

It should be noted that the entire analysis described above did not involve the actual solution of the equations of motion. Therefore, four parameters are required as input in order to enable calculations. These are: C_f, ϕ_w, Re_δ, and β_e. In addition, the determination of γ_m requires knowledge of the external flowfield. In a real situation these would be unknowns, and the equations of motion would have to be solved, subject to a prescribed pressure distribution and initial velocity profile. However, regardless of the method of solution, the above model then could be incorporated into the solution scheme, since it does not introduce any additional unknowns of its own.

Comparison with Experimental Data

The data of Refs. 4 and 6 have been used to check the validity of the proposed models for the wall and wake laws. Both sources of data use flow geometries which lead to a buildup of adverse pressure gradient with eventual three-dimensional separation. The measurement stations chosen for comparison between theory and data were all fully attached. Results of two stations from Ref. 4 and three from Ref. 6 are reported here: in station C4 in Ref. 6 an 8% crossflow is present, in station D5 the crossflow is about 12%, and in

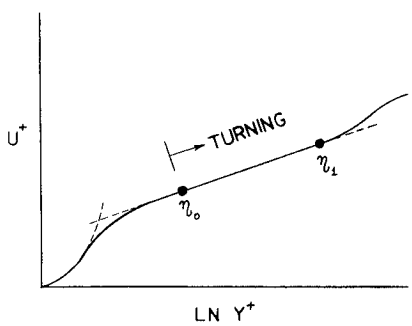

Fig. 5 Schematic of a velocity plot showing the relation of η_1 to η_0.

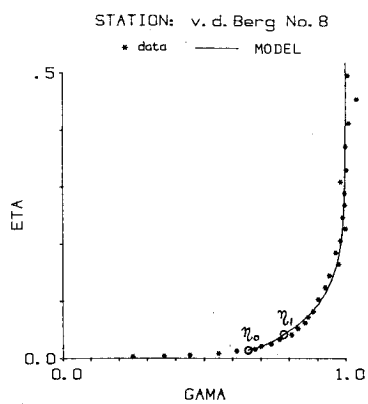

Fig. 6 Comparison between the model for $\Gamma(\eta)$ and experimental data of Ref. 4, station 8 (the five lowest points belong to the wall sublayer).

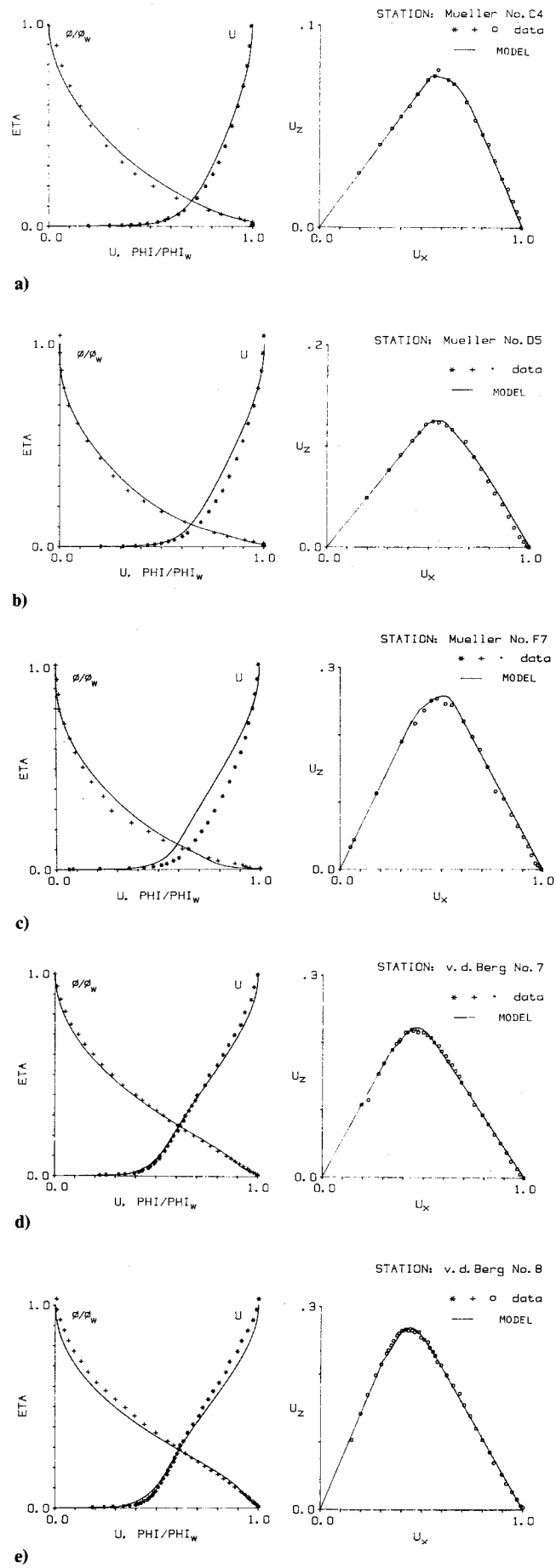

Fig. 7 Comparison between model and experimental data of selected measurement stations from Refs. 4 and 6 (shown are resultant velocity in magnitude and direction, and the velocity hodograph).

station F7 it reaches about 25% of the streamwise flow component. In station 7 of Ref. 4 the crossflow is about 22% and in station 8 it reaches 27%. Figures 7a-e show comparisons between the present theory and the data of the representative measurement stations. The figures include comparisons for both the hodograph and the resultant velocity profile (in terms of magnitude and direction). The agreement is good for all stations. In particular, it is noted that the theory is able to predict the smooth transition from wall to the wake region.

Comparison with Johnston's Triangular Model

Johnston[2] assumed the following model for the $U_z = U_x$ hodograph:

$$U_z = U_x \tan\phi_w, \qquad U_x \le U_p$$

$$= A(1-U_x), \qquad U_x > U_p$$

In contrast, the present model assumes no geometric relationship. Rather, the hodograph results on the basis of the fundamental assumption that the wake function is a vector quantity. In comparing the two models, it is observed that the first leg of Johnston's triangle corresponds to the wall law of the present model, while the second leg corresponds to a special case of the present model's wake law, namely, $\Gamma = 1$ with $A = \tan\gamma_m$. However, this is an inadequate choice since it fails to correctly describe either the transition from the wall to the wake region or the magnitude and location of the maximum crossflow (see Fig. 4). These shortcomings are apparent from Johnston's own polar plots (see Ref. 2). The other basic difference between the two models stems from the fact that whereas Johnston regards the vertex of his triangle as the edge of the wall sublayer, the present model locates this point at η_0, corresponding to γ_0 (see Fig. 4).

Conclusions

An asymptotic analysis has been carried out for three-dimensional, pressure-driven turbulent boundary layers. This analysis indicates that, as in the two-dimensional case, the flow is multistructured, possessing inner (wall), middle (defect), and outer layers. The inner layer, which is exponentially thin compared to the middle layer, is dominated by constant total shear across it, inertia and pressure gradients having no significant influence there. The middle layer is driven both by the pressure gradient and the Reynolds stresses, and may be described by boundary-layer-type equations. These two sublayers have a common logarithmic overlap region. The outer layer is inviscid and generally rotational, describable by the Euler equations.

These results indicate that the wall sublayer is two-dimensional, flowing in the local wall shear direction, and all the turning from this direction to the freestream direction takes place in the defect layer.

Based on these results, a model is proposed for the three-dimensional counterpart of the law of the wall and law of the wake, which agrees very well with experimental data.

Appendix: Determination of the Function $\gamma(\eta)$

From the law of the wall, Eq. (3), one gets

$$\frac{d\tilde{U}}{d\tilde{Y}} = \frac{u_\tau^2}{\nu}\frac{df}{dy^+} \tag{A1}$$

From the law of the wake, Eq. (7), one gets

$$\frac{d\tilde{U}}{d\tilde{Y}} = \frac{u_\tau^2}{\delta\tilde{U}}\left[F\frac{dF}{d\eta} - \lambda\left(\frac{dF}{d\eta}\cos\gamma - F\sin\gamma\frac{d\gamma}{d\eta}\right)\right] \tag{A2}$$

Multiplying both expressions by $\tilde{Y}/u_\tau$ and equating, yields

$$y^+\frac{df}{dy^+} = \frac{\eta}{U}\left[\left(\frac{F}{\lambda} - \cos\gamma\right)\frac{dF}{d\eta} + F\sin\gamma\frac{d\gamma}{d\eta}\right] = \kappa^{-1} \tag{A3}$$

Since the left-hand side is a function of y^+ only and the right-hand side of η only (these are independent variables in the context of asymptotic analysis), both are equal to the same constant, κ^{-1}. Integration of the left-hand side yields $f = \kappa^{-1}\ell n y^+ + B$, which is the logarithmic overlap expressed in terms of wall variables. Substituting Eq. (6) into the right-hand side of Eq. (A3) yields

$$\frac{\eta}{U}\left[\left(\frac{F_{2D}}{\lambda\cos^2\gamma} - 1\right)\frac{dF_{2D}}{d\eta} + \frac{F_{2D}^2\tan\gamma}{\lambda\cos^2\gamma}\frac{d\gamma}{d\eta}\right] = \kappa^{-1}$$

from which

$$\frac{d\gamma}{d\eta} = \frac{\lambda\cos^2\gamma}{F_{2D}^2\tan\gamma}\left[\frac{U}{\kappa\eta} - \left(\frac{F_{2D}}{\lambda\cos^2\gamma} - 1\right)\frac{dF_{2D}}{d\eta}\right] \tag{A4}$$

where U is given by Eq. (7) and F_{2D} by Eq. (4). The initial condition required for the solution of Eq. (A4) is determined as follows: according to the asymptotic analysis the hodograph (Fig. 4) starts deviating from the ϕ_w direction at the point in the logarithmic overlap where the wall and wake velocity vectors are in the same direction. This point is designated as η_0.

From Fig. 4,

$$u^+ = \lambda\Big/\left(\cos\phi_w + \frac{\sin\phi_w}{\tan\gamma}\right) \tag{A5}$$

Combining this with Eqs. (6) and (8) yields

$$\tan\phi(\eta) = \sin\phi_w\Big/\left\{\left[\frac{\lambda}{u^+(y^+)} - \cos\phi_w\right]\left[\frac{\lambda}{F_{2D}(\eta)} - 1\right]\right\} \tag{A6}$$

in the logarithmic overlap. Here,

$$y^+ \equiv \frac{Re_\delta}{\lambda}\eta$$

and u^+ and F_{2D} are given by Eqs. (3) and (4), respectively. Equation (A6) is solved iteratively[9] for η_0 which is the largest η for which $\phi(\eta) = \phi_w$. γ_0 is then found from Eq. (8) with $\eta = \eta_0$ and $\phi = \phi_w$. This determines the required initial conditions for Eq. (A4), the solution of which provides $\gamma(\eta)$ in the logarithmic overlap region, which is the lower portion of the $\gamma(\eta)$ curve.

At the upper portion of the defect layer $\gamma = \gamma_m$ [Eq. (11)]. To complete the formulation of γ, it is necessary to devise a curve fit which smoothly connects the lower and upper portions of the $\gamma(\eta)$ curve. To this end one defines the function

$$\Gamma \equiv \frac{\gamma}{\gamma_m} = 1 - \beta(1-\eta)^\alpha \tag{A7}$$

The following requirements are necessary to be met by this function:

$$\Gamma(1) = 1, \quad \frac{d\Gamma}{d\eta} > 0, \quad \lim_{\eta\to 1}\frac{d\Gamma}{d\eta} = 0, \quad \frac{d^2\Gamma}{d\eta^2} < 0, \quad \lim_{\eta\to 1}\frac{d^2\Gamma}{d\eta^2} = 0$$

(zero curvature as $\eta \to 1$).

These requirements are met provided that $\alpha > 2$ and $\beta > 0$. The latter two parameters are determined by matching Γ to the curve described by Eq. (A4) at a matching point η_1, where the velocity profile switches from the logarithmic overlap to

the wake (see Fig. 5):

$$\Gamma = \frac{\gamma_1}{\gamma_m} \qquad \text{at } \eta = \eta_1$$

$$\frac{d\Gamma}{d\eta} = \gamma_m^{-1} \frac{d\gamma}{d\eta} \qquad \text{at } \eta = \eta_1$$

where $\gamma(\eta)$ is the function at the logarithmic overlap region, and γ_1 is its value at $\eta = \eta_1$. From this one gets

$$\alpha = \frac{1-\eta_1}{1-\Gamma_1} \frac{d\Gamma}{d\eta}\bigg|_{\eta=\eta_1} \tag{A8}$$

and

$$\beta = \frac{1-\Gamma_1}{(1-\eta_1)^{\alpha}} \tag{A9}$$

η_1 is generally a function of Re_δ and pressure gradient. Based on experimental data, a typical value for it is 0.035.

References

[1] Coles, D. E., "The Law of the Wake in the Turbulent Boundary Layer," *Journal of Fluid Mechanics*, Vol. 1, Pt. 2, 1956, pp. 191-226.

[2] Johnston, J. P., "On the Three-Dimensional Turbulent Boundary Layer Generated by Secondary Flow," *Journal of Basic Engineering*, Vol. 82, March 1960, pp. 233-248.

[3] Mellor, G. L., "The Large Reynolds Number, Asymptotic Theory of Turbulent Boundary Layers," *International Journal of Engineering Science*, Vol. 10, Oct. 1972, pp. 851-873.

[4] Berg, B. van den and Elsenaar, A., "Measurements in a Three Dimensional Incompressible Turbulent Boundary Layer in an Adverse Pressure Gradient under Infinite Swept Wing Conditions," NLR Tech. Rept. 72092U, 1972.

[5] Berg, B. van den, Elsenaar, A., Lindhout, J.P.F., and Wesseling, P., "Measurements in an Incompressible Three-Dimensional Turbulent Boundary Layer, under Infinite Swept-Wing Conditions, and Comparison with Theory," *Journal of Fluid Mechanics*, Vol. 70, Pt. 1, 1975, pp. 127-148.

[6] Mueller, U. R., "Mean Velocities and Reynolds Stresses Measured in a Three-Dimensional Boundary Layer," AFFDL Tech. Rept. 80-3088, 1980, p. 359.

[7] Mueller, U. R., "Measurement of the Reynolds Stresses and the Mean Flow Field in a Three-Dimensional Pressure-Driven Boundary Layer," *Journal of Fluid Mechanics*, Vol. 119, June 1982, pp. 121-153.

[8] Musker, A. J., "Explicit Expression for the Smooth Wall Velocity Distribution in a Turbulent Boundary Layer," *AIAA Journal*, Vol. 17, June 1979, pp. 655-657.

[9] Dowell, M. and Jarratt, P., "The 'Pegasus' Method for Computing the Root of an Equation," *BIT*, Vol. 12, 1972, pp. 503-508.